Journal of Applied Mechanics and Technical Physics, Vol. 37, No. 4, 1996

EXPERIMENTAL INVESTIGATION OF CURRENT INSTABILITY OF SHAPED-CHARGE JETS

A. D. Matrosov and G. A. Shyetsov

UDC 532.52+533.95

Introduction. The hydrodynamic theory of the formation of shaped-charge jets was developed by M. A. Lavrent'ev [1, 2] and Birkhoff with coworkers [3]. M. A. Lavrent'ev noted [2] that, in the operation of a shaped charge with an arbitrary pulse distribution, different parts of the jet can move with different velocities. During flight, some sections of the jet are compressed and the other sections are stretched. The instability of a shaped-charge jet results in a decrease in the penetration depth as the charge recedes from the target. For conical shells, the jet tip velocity reaches 10 km/sec and the jet temperature is about 500–900°C [4, 5]. Flash radiography has shown that the velocity gradient from the tip to the tail is almost always uniform. This velocity gradient causes the jet to stretch. Because of this stretching, series of surface disturbances develop along the jet and result in break of the jet into separate fragments.

In the present paper, we present the results of an experimental study of the behavior of shaped-charge jets with passage of an axial electric current through them. It is found that in excess of certain values of the current, current derivative, and the time of electromagnetic action, shaped-charge jets begin to break into separate fragments. Shaped charges with conical copper liners with diameters of from 30 to 100 mm were used in the tests. The failure of shaped-charge jets remained qualitatively the same for charges of different diameters. In the authors' opinion, this is due mainly to the accelerated growth in the initially small perturbations of the shape of the lateral surface of the shaped-charge jet under electromagnetic action. The accelerated development of necking instability in experiments with current results in an earlier break of the shaped-charge jet into fragments as compared with the time of fracture of the jet without current. The experimental results presented in the paper were obtained in late 1970s to the early 1980s.

Physical Prerequisites. Before proceeding to a description of the experimental diagram and results we make several preliminary remarks.

(1) The interaction of the current flowing over a conductor with the magnetic field of the latter produces radial and axial forces whose action leads to compression of the conductor in the radial direction and simultaneous (in the presence of neckings) compression and stretching in the axial direction (Fig. 1). It should be noted that the magnetic pressure $p = B^2/2\mu_0 = \mu_0 I^2/8\pi^2 r^2$ (B is the induction of the magnetic field, I is the electric current, μ_0 is the magnetic permeability of vacuum, and r is the jet radius) in the necking zone can be much greater than the magnetic pressure in the zones of convexity.

(2) Let us define the magnitude of the magnetic field for which magnetic pressure produces mechanical stresses in metal that correspond to the yield strength Y as the yield field $B_Y = \sqrt{2\mu_0 Y}$. For a number of materials the magnitudes of the yield fields and the corresponding linear current densities I/r on the surface of cylindrical conductors are presented in Table 1. The physical meaning of B_Y is obvious. For $B < B_Y$, elastic deformations occur; for $B > B_Y$, plastic deformations take place. In the latter case one would expect accelerated growth of neckings and breakup of metallic shaped-charge jets under relatively low currents.

It should be noted that the values of B_Y and $(I/r)_Y$ presented in Table 1 should be regarded only as estimates, because they are obtained for static values of the yield strength at 20°C [6]. To estimate the

Lavrent'ev Institute of Hydrodynamics, Siberian Division, Russian Academy of Sciences, Novosibirsk 630090. Translated from Prikladnaya Mekhanika i Tekhnicheskaya Fizika, Vol. 37, No. 4, pp. 9–14, July–August, 1996. Original article submitted April 25, 1995.

 0021-8944/96/3704-0464 $15.00

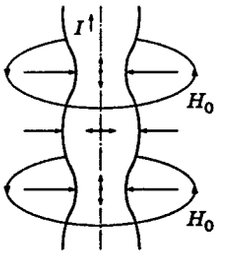

Fig. 1

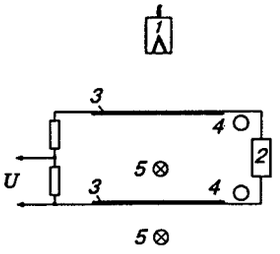

Fig. 2

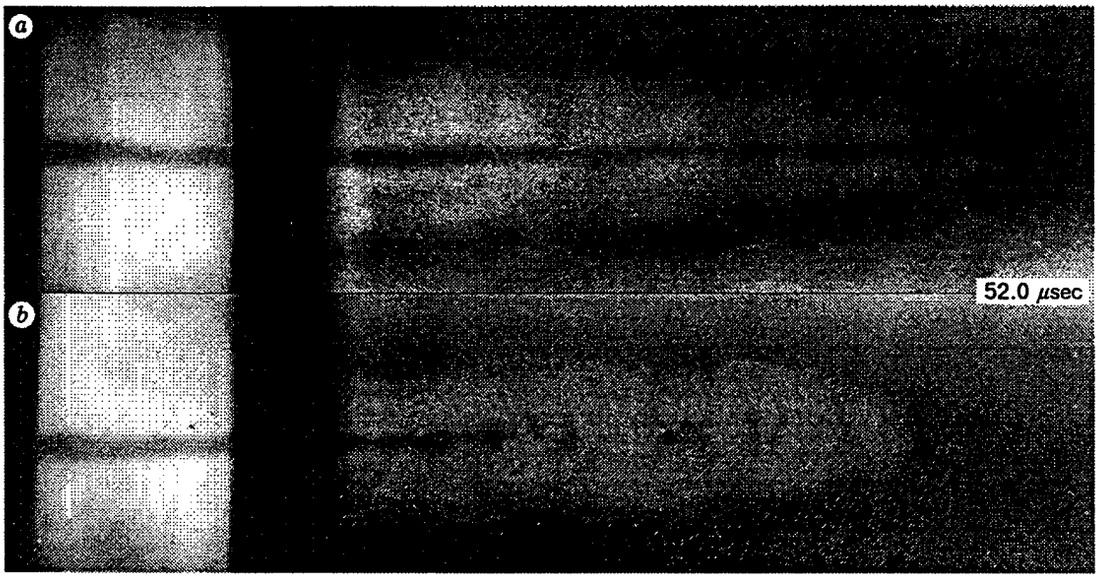

Fig. 3

yield field in the case of a shaped-charge jet, one should use the dynamic yield strengths of materials, which are known to be somewhat higher than the static yield strengths, and take into account the dependence of the yield strength on the initial jet temperature. By way of example, we note that at 600–1,000°C the yield strength of copper decreases by a factor of 5–20 [7]. Accordingly, one might expect a severalfold decrease in the values of B_Y and $(I/r)_Y$.

If the above remarks and estimates are valid, the yield strength is only a few percent of the magnetic pressure for currents of $(3\text{–}5) \cdot 10^5$ A and $r_0 = 1$ mm (r_0 is the mean radius). Under these conditions, a shaped-charge jet can be considered an incompressible, conducting, perfectly plastic fluid.

Diagram of the Experiment. The diagram of the experiments is shown in Fig. 2, where 1 is the shaped charge, 2 is the magnetic-energy source, 3 are the electrodes, 4 are the inductive probes used to measure current and the discharge-current derivative, and 5 are the places of x-ray photography. Shaped charges with conical copper liners with diameters of from 30 to 100 mm were used in the experiments. A capacitor bank with a charging voltage of up to 5 kV and a capacity of up to 20 mF was used as an energy source. The current starts to flow in the shaped-charge jet when the jet closes the electrodes. Current, discharge current derivative (100–500 kA, $3 \cdot 10^9$–10^{11} A/sec), the electric-pulse time, the time of action on the various parts of the jet, and other parameters were varied in the tests. Radiography of the shaped-charge jet in free flight and in the target (aluminum) was carried out by a PIR-100/240 flash radiograph with an exposure of approximately 100 nsec. In experiments with and without current, the accuracy of flash radiography was not worse than 0.5

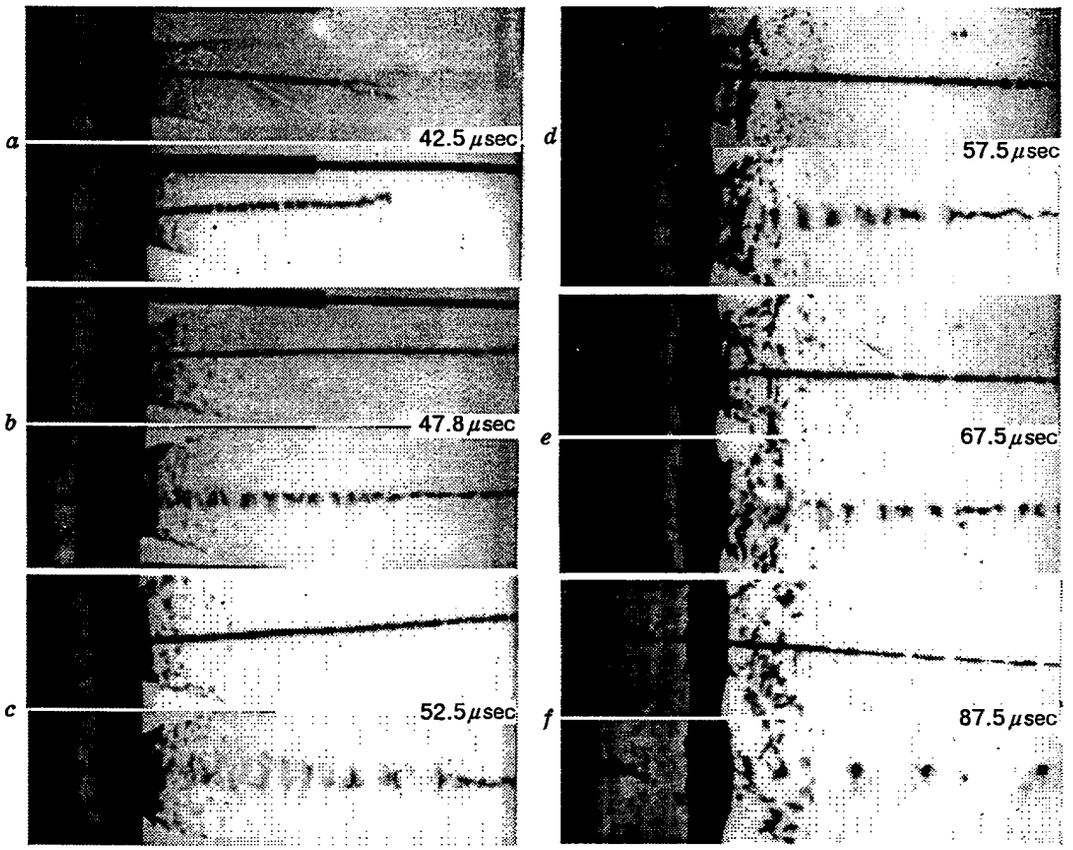
a
42.5 μsec
b
47.8 μsec
c
52.5 μsec
d
57.5 μsec
e
67.5 μsec
f
87.5 μsec

Fig. 4

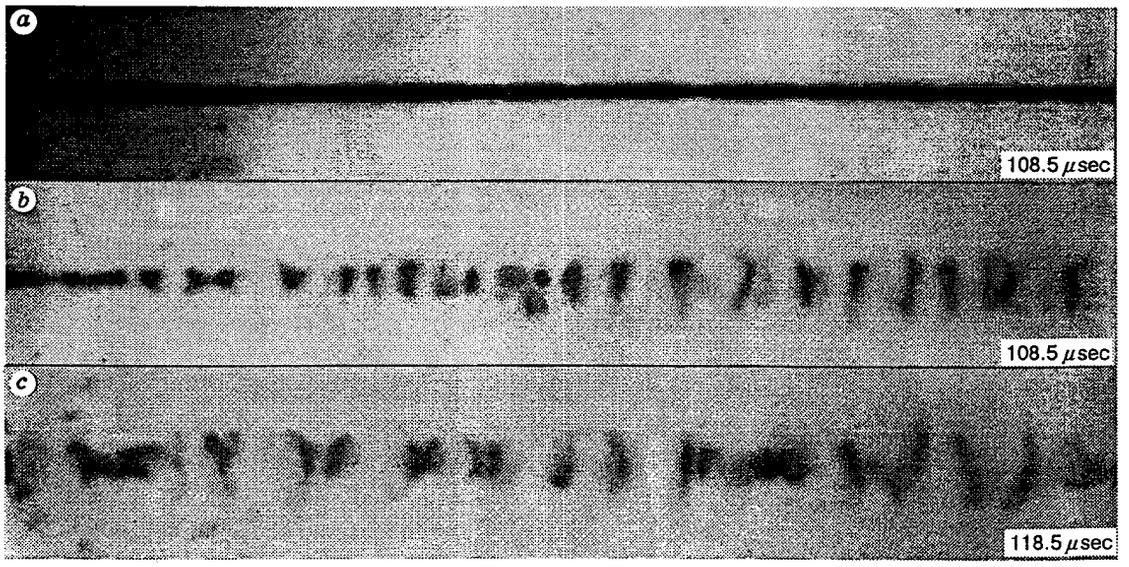
a
108.5 μsec
b
108.5 μsec
c
118.5 μsec

Fig. 5

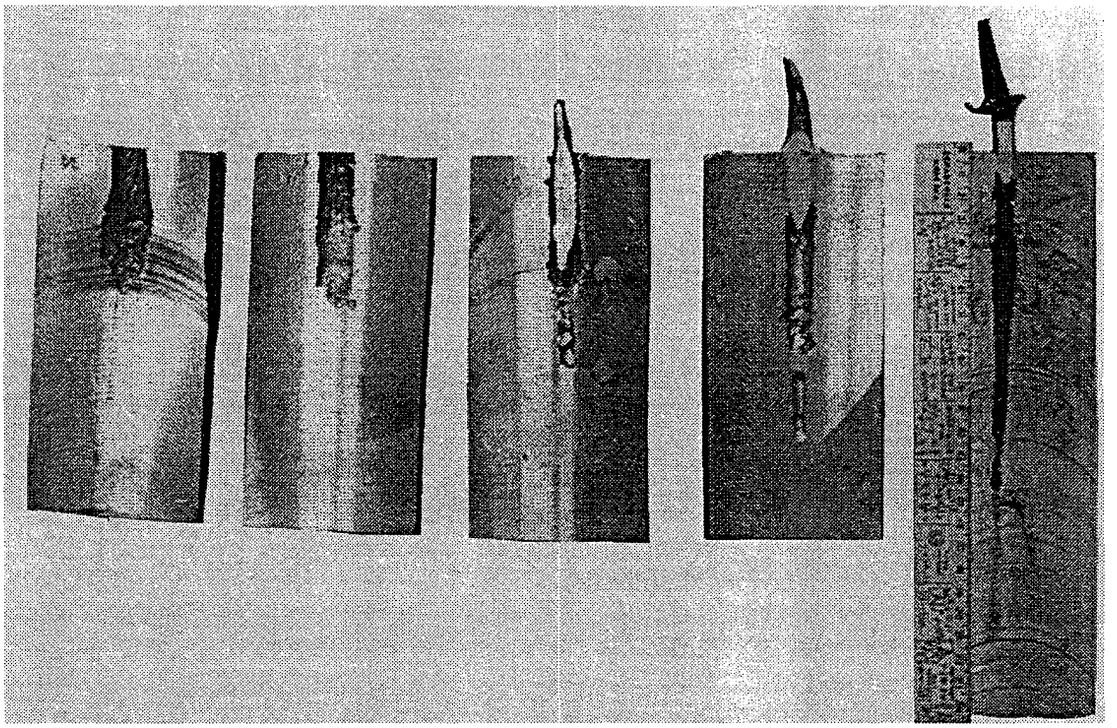

Fig. 6

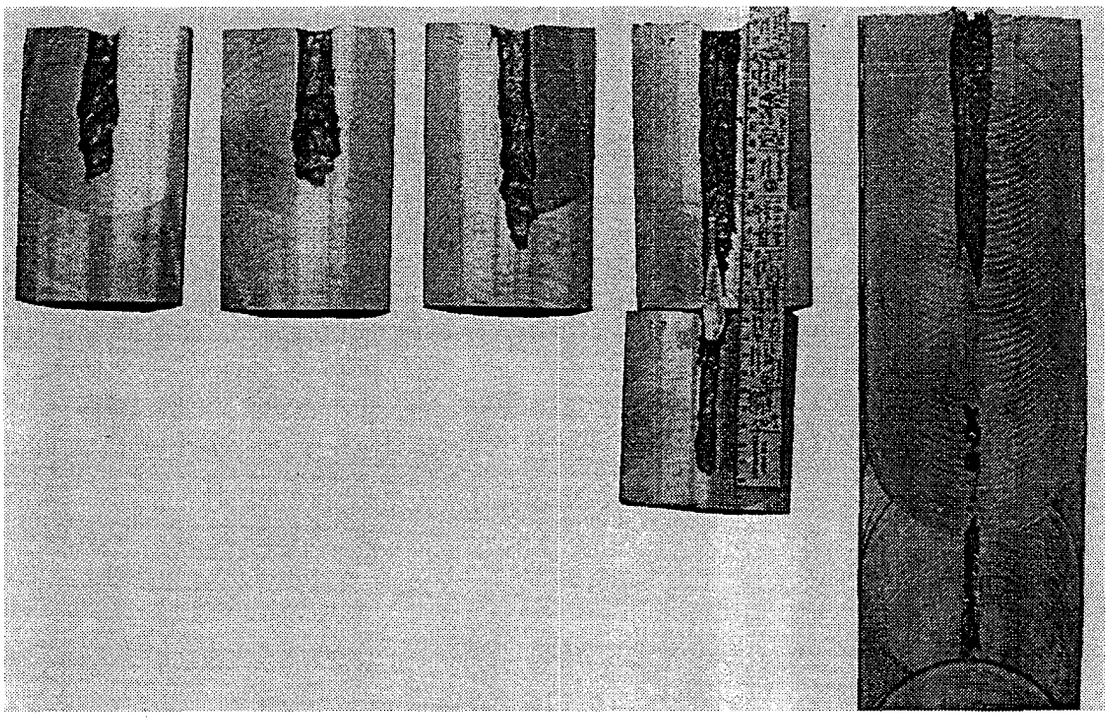

Fig. 7

TABLE 1

Material	$Y \cdot 10^9$, Pa	B_Y, T	$(I/r_0)_Y$, kA/mm
Aluminum (annealed)	0.022	7.4	37.3
Silver (annealed)	0.02–0.03	7.9	39.7
Copper (annealed)	0.07	13.3	66.5
Copper	0.2	22.6	112.3
Nickel (annealed)	0.08	14.2	71.1
Titanium (extrapure)	0.1	15.8	79.4
Iron (annealed)	0.17	20.7	103.6
Steel 3	0.22	23.8	119.2
Tantalum (annealed)	0.4	31.8	158.9
Molybdenum (annealed)	0.57	37.7	189.7
Tungsten (deformed)	0.76	43.9	219.0

μsec at the same time. The effect of electric current on the shaped-charge jet was additionally judged from jet penetration into the target.

Experimental Results. Figure 3 shows radiographs of two tests with 50-mm shaped charges [experiment without current (a) and experiment with a current of 450 kA (b)]. An aluminum target was one of the electrodes. The cavern depths were approximately equal at the moment of filming. In the experiment with current the jet broke into individual fragments.

Figure 4 shows pairs of radiographs of a jet with current and without current made at different times. One can see from the radiographs beginning with Fig. 4b that in experiments with a current shaped-charge jets have discontinuities in front of the lower electrode with noticeable thickening of the jet diameter above the discontinuities. After passing the lower electrode, the jet breaks into individual fragments whose sizes in the axial direction are approximately equal to 1–3 jet diameters. The fragments stretch in the radial direction to reach 5–10 jet diameters in the same cross sections as in experiments without current. The failure patterns of shaped-charge jets from charges with diameters of 30, 50, and 100 mm is qualitatively the same. Figure 5 gives radiographs of the jets from 100-mm shaped charges [experiment without current (a) and experiment with a current (b and c)].

Analysis of radiographs that were taken at the same times shows that the number of neckings in the jet without current and the number of fragments in experiments with a current coincides fairly well. Figure 5a shows ten visible neckings and Fig. 5b eleven fragments on the same base.

The above catastrophic behavior of shaped-charge jets with passage of an electric current through them leads to a severalfold decrease in the cavern depth in the target. This process can be controlled by varying the current amplitude, the time of build-up, and the duration of the electric pulse. Figures 6 and 7 present cavern depths in steel and aluminum targets, respectively, versus the discharge current amplitude for the same current derivative and electric-pulse duration.

Thus, the studies performed show that shaped-charge jets are unstable in the magnetic field of an axial current. The effects arising in a shaped-charge jet with passage of a current through it are of interest from both practical (decrease in jet penetration into the target) and methodical viewpoints (in studies of the material behavior and physical characteristics of shaped-charge jets).

REFERENCES

1. M. A. Lavrent'ev, "Fundamentals of the theory of shaped charges and their armor-piercing action," *Izv. Artiller. Akad.*, **56**, 3–21 (1948).
2. M. A. Lavrent'ev, "A shaped-charge jet and its operating principle," *Usp. Mat. Nauk*, **12**, No. 4, 41–56 (1957).

3. G. Birkhoff, D. MacDougall, E. Pugh, and G. Taylor, "Explosives with lined cavities," *J. Appl. Phys.*, **19**, No. 6, 563–582 (1948).
4. K. P. Stanukovich (ed.) *Physics of Explosion* [in Russian], Nauka, Moscow (1975).
5. W. P. Walters and J. A. Zukas, *Fundamentals of Shaped Charges*, John Wiley and Sons, New York (1989).
6. I. S. Grigor'ev and E. Z. Melikhov (eds.), *Physical Quantities*: Handbook [in Russian], Energoatomizdat (1981).
7. A. A. Presnyakov, *Localization of Plastic Deformation* [in Russian], Nauka KazSSR, Alma-Ata (1981).